Proc. Natl. Acad. Sci. USA
Vol. 96, pp. 7962–7967, July 1999
Cell Biology

Nephrin is specifically located at the slit diaphragm of glomerular podocytes

VESA RUOTSALAINEN*†, PÄIVI LJUNGBERG*‡§, JORMA WARTIOVAARA¶, ULLA LENKKERI†, MARJO KESTILÄ†, HANNU JALANKO‡, CHRISTER HOLMBERG‡, AND KARL TRYGGVASON†‖

†Biocenter and Department of Biochemistry, University of Oulu, 90570 Oulu, Finland; ‡Hospital for Children and Adolescents, University Hospital of Helsinki, 00014 Helsinki, Finland; §Department of Bacteriology and Immunology, Haartman Institute and ¶Electron Microscopy Unit, Institute of Biotechnology, University of Helsinki, 00014 Helsinki, Finland; and ‖Division of Matrix Biology, Department of Medical Biochemistry and Biophysics, Karolinska Institute, 171 77 Stockholm, Sweden

Communicated by Peter A. Reichard, Karolinska Institute, Stockholm, Sweden, April 9, 1999 (Received for review February 12, 1999)

ABSTRACT **We describe here the size and location of nephrin, the first protein to be identified at the glomerular podocyte slit diaphragm. In Western blots, nephrin antibodies generated against the two terminal extracellular Ig domains of recombinant human nephrin recognized a 180-kDa protein in lysates of human glomeruli and a 150-kDa protein in transfected COS-7 cell lysates. In immunofluorescence, antibodies to this transmembrane protein revealed reactivity in the glomerular basement membrane region, whereas the podocyte cell bodies remained negative. In immunogold-stained thin sections, nephrin label was found at the slit between podocyte foot processes. The congenital nephrotic syndrome of the Finnish type (NPHS1), a disease in which the nephrin gene is mutated, is characterized by massive proteinuria already *in utero* and lack of slit diaphragm and foot processes. These features, together with the now demonstrated localization of nephrin to the slit diaphragm area, suggests an essential role for this protein in the normal glomerular filtration barrier. A zipper-like model for nephrin assembly in the slit diaphragm is discussed, based on the present and previous data.**

Ultrafiltration of blood during formation of the primary urine in the glomerulus is one of the central functions of the human kidney (1). Structurally, the glomerulus is a tuft of anastomosing capillary loops surrounded by the Bowman's capsule leading the primary urine to the tubular system. The glomerular filtration barrier is formed by three layers: the innermost fenestrated vascular endothelium, the glomerular basement membrane (GBM), and the podocyte layer. The podocytes form a tight web on top of the GBM with their interdigitating foot processes joined by a slit diaphragm.

It is generally acknowledged that the molecules passing through the glomerular filtration barrier are selected according to their size, charge, and shape (2–8). The exact locations of the various selective functions in the barrier are, however, more controversial. The charge-selective filter has been thought to be located in the GBM, a crosslinked meshwork of type IV collagen, laminin, nidogen, and proteoglycans (9, 10). The anionic charge of heparan sulfate side chains of proteoglycans is believed to hinder the traversal of anionic plasma proteins (5, 11, 12). The location of the size-selective property of the filtration barrier has been attributed to the GBM alone or, alternatively, to the slit diaphragm (5, 13, 14).

Concerning the molecular composition of the slit diaphragm, monoclonal antibody 5–1-6 (15) that recognizes a 51-kDa protein has been shown in immunoelectron microscopy to react exclusively with the slit diaphragm (16). However, the nature of this protein is still unknown. The α-isoform of the tight junction protein ZO-1 (17) has been localized in the glomerulus, predominantly to points where the slit diaphragm is inserted into the lateral cell membrane of the foot process (18). The ZO-1 protein possibly connects the slit diaphragm, directly or indirectly, to the cytoskeleton.

In numerous primary and secondary diseases of the kidney, the filtration barrier is affected, resulting in proteinuria, i.e., leakage of albumin and larger plasma proteins into the urine, with edema and nephrotic syndrome as a consequence. Many cases also include an immunological component in their etiology which, however, is not the case in the congenital nephrotic syndrome of the Finnish type (NPHS1) (19). We have recently identified the gene mutated in NPHS1 (20, 21). The disease specifically affects the kidney and is characterized by massive proteinuria already *in utero*. Electron microscopic examination of NPHS1 patient kidneys reveals thinner lamina densa of the GBM than in controls, but no structural abnormality of the GBM has been detected (22, 23). In kidneys of patients with NPHS1, the podocyte foot processes are absent, and no slit diaphragms have been described in the podocyte cell–cell adhesions. This finding is typical for nephroses of any cause.

The gene mutated in NPHS1 codes for a putative transmembrane protein termed nephrin that belongs to the Ig superfamily. It has an extracellular portion containing eight Ig motifs and one type III fibronectin domain (20). These properties, together with the sequence of the intracellular domain that contains eight tyrosines, suggested that nephrin is a signaling adhesion molecule. By using *in situ* hybridization, nephrin was shown to be exclusively expressed in glomerular podocytes (20).

In the present study, we localized nephrin in immunofluorescence microscopy to the GBM region of newborn human glomeruli, using antibodies generated against recombinant antigen. Moreover, we demonstrated by immunoelectron microscopy that nephrin is located in the podocyte slit region. We propose that nephrin is most likely a component of the slit diaphragm. The fact that the protein is mutated in NPHS1 further indicates an essential role for the slit diaphragm in the maintenance and size selectivity of the glomerular filtration barrier.

MATERIALS AND METHODS

Generation and Characterization of Antiserum. The N-terminal fragment of nephrin was produced in *Escherichia coli* by using the QiaExpressionist kit from Qiagen. The cDNA-

The publication costs of this article were defrayed in part by page charge payment. This article must therefore be hereby marked "*advertisement*" in accordance with 18 U.S.C. §1734 solely to indicate this fact.

PNAS is available online at www.pnas.org.

Abbreviation: GBM, glomerular basement membrane.

Data deposition: The sequence reported in this paper has been deposited in the GenBank database (accession no. AF035835).

*These authors contributed equally to this work.

‖To whom reprint requests should be addressed. e-mail: karl.tryggvason@mbb.ki.se.

encoding amino acids 22 to 240 (21) were amplified from human fetal kidney 5′STRETCH cDNA library (CLONTECH) by PCR. Synthetic oligonucleotides were used to generate additional restriction sites *Bgl*II (5′) and *Hin*dIII (3′) to the ends of the cDNA to facilitate cloning into *Bam*HI/*Hin*dIII-digested vector pQE-30. Production and initial purification of the six-histidine-tagged protein on Ni-NTA column was carried out according to the manufacturer's instructions. Protein was purified under denaturing conditions in phosphate buffer containing 8 M urea. For further purification, the protein was diluted 10-fold with an anion exchange chromatography buffer (8 M urea,/0.05 M Tris/1 mM dithiotreitol, pH 8) and purified on Source Q column (Amersham Pharmacia Biotech) by using a linear NaCl-gradient. Protein was precipitated by dialysis against PBS. The precipitate was solubilized in 1% SDS, diluted 10-fold with PBS, and used as an antigen to raise polyclonal antibodies in rabbits by using standard procedures (SLA, Uppsala, Sweden). The antisera were characterized by using Western blotting, ELISA, and immunofluorescence microscopy.

Purification of Antibodies. For immunolocalization studies, rabbit IgG was affinity purified with protein A Sepharose FF (Amersham Pharmacia Biotech). For Western blot analysis, the antibody was purified by using nitrocellulose-bound recombinant antigen (24). Briefly, 2 μg of antigen was separated by preparative SDS gel electrophoresis and blotted onto nitrocellulose membrane. The antigen-containing band was cut into pieces and blocked with BSA. Antiserum was diluted 10-fold with TBS (0.05 M Tris/0.15 M NaCl, pH 7.5) and incubated with membrane pieces for 2 hr at room temperature. After four washings with TBS, bound antibodies were eluted with 0.1 M glycine, pH 3.5.

Western Blotting. From isolated glomeruli, the proteins were extracted into sonication buffer (0.05 M sodium phosphate/0.15 M NaCl/1% Triton X-100/0.1 mM phenylmethylsulfonyl fluoride/10 mM ethylenediaminetetraacetic acid, pH 7.5). Samples were treated with or without 10 mM dithiotreitol in sonication buffer. After brief sonication, the samples were incubated on ice for 30 min and centrifuged to clear the supernatant. For SDS/PAGE, the lysates were diluted in Laemmli sample buffer (25), with or without 5% 2-mercaptoethanol, and run on a 6% gel. COS-7 cells transiently expressing nephrin were treated similarly, except that the reduction was done only before electrophoresis with mercaptoethanol.

SDS/PAGE and Western blot analyses were performed according to standard methods (25, 26). Proteins were transferred onto poly(vinylidene difluoride) membrane and blocked with 1% BSA in tris-buffered saline. After anti-nephrin or preimmune IgG-incubation (0.1 μg/ml), primary antibodies were detected with horseradish peroxidase-conjugated anti-rabbit IgG (Dako) and chemiluminescent reagent (ECLplus, Amersham Pharmacia Biotech).

Cloning of Full Length Nephrin cDNA and Expression in COS-7 Cells. A 2.4-kb PCR fragment was amplified from a fetal kidney cDNA library with primers selected from exons 1 and 17. This PCR product was then used as a probe to screen the library for full length cDNA. One clone was subcloned as two separate *Eco*RI fragments into pBluescript (Stratagene). PCR was used to introduce *Bgl*II restriction site upstream of the putative ATG initiator methionine site to facilitate cloning into the *Bam*HI/*Eco*RI-digested expression vector pcDNA3 (Invitrogen). The construct was sequenced and transfected into the COS-7 cell line by using the Fugene-6 transfection reagent (Boehringer Mannheim). These transiently transfected cells were used to characterize polyclonal antiserum with immunofluorescence microscopy and Western blotting.

Indirect Immunofluorescence Microscopy. Cryosections 5–10 μm thick from a 2-mo-old infant were placed on gelatin-coated slides and dried at room temperature. Sections were fixed in ethanol for 10 min at room temperature and washed in PBS. Cultured cells were fixed with 4% paraformaldehyde for 3 min and then with ethanol for 10 min at room temperature. To block nonspecific binding, the samples were incubated in 10% horse serum in PBS for 30 min at room temperature. Rabbit primary antisera were used at dilutions 1:200 to 1:400 in 1% horse serum in PBS. Incubations were carried out for 2 hr at 37°C or overnight at 4°C.After washings in PBS, the primary antibody was detected by using FITC-labeled anti-rabbit IgG antibody (Dako) at dilution 1:200 for 60 min at 37°C. After washings in PBS, the sections were analyzed with fluorescence microscopy.

Immunoelectron Microscopy. Kidney tissue from three brain-dead intended donors (a 49-yr-old female unsuitable as donor because of being positive for hepatitis B surface antigen, a 30-yr-old female who was found to have variation in the kidney vasculature, and a normal 17-yr-old male whose kidney was biopsied) were processed for postembedding immunoelectron microscopy. The kidneys had been stored in ViaSpan solution (DuPont Merck) for 12, 15, and 24 hr, respectively, until processing. Cubicles ($1 \times 1 \times 5$ mm) were cut with a razor blade from the renal cortex in PBS. The samples were fixed in 3.5% paraformaldehyde (Sigma) alone or combined with 0.01% glutaraldehyde (Electron Microscopy Sciences, Fort Washington, PA) in 0.1 M phosphate buffer (pH 7.3) at room temperature for 1, 1.5, and 19 hr, respectively. Fixed samples were washed in phosphate buffer, dehydrated in graded ethanol, and embedded in LR white (London Resin, Basingstoke, U.K.) and Lowicryl K4M (Polysciences) resins.

Thin sections were cut on Pioloform (Agar Scientific, Stansted, Essex, U.K.) and carbon-coated nickel grids. For indirect immunostaining, the grids were incubated in the first antibody diluted in 3% BSA/PBS (1:100–200 for rabbit anti-nephrin whole serum and to 10–50 μg/ml for the protein A affinity-purified rabbit anti-nephrin IgG) for 60 min. Grids were then treated with the second antibody [10 nm colloidal gold goat anti-rabbit F(ab)$_2$, British BioCell, Cardiff, U.K., or 6 nm colloidal gold–affinipure goat anti-rabbit IgG (Jackson ImmunoResearch)], diluted in 3% BSA/PBS (1:50 or 1:30) for 30 min at room temperature. The sections were examined under a Jeol 1200 EX electron microscope at 60 kV accelerating voltage.

RESULTS

Characterization of Polyclonal Nephrin Antibodies. Rabbit antiserum made against recombinant Ig repeats 1 and 2 of the amino terminal extracellular portion of human nephrin was shown to specifically react with full length recombinant nephrin in Western blot analysis (Fig. 1). Antibodies were also shown to be reactive in ELISA against the antigen, as well as in immunofluorescence microscopy against COS-7 cells transfected with full length nephrin cDNA. Mock-transfected cells did not yield immunoreactivity (data not shown). The antiserum reacted with a 180-kDa protein present in Triton X-100 extracts of human glomeruli (Fig. 1). Full length recombinant nephrin produced in COS-7 cells has a smaller size of ≈150 kDa. The sequence-predicted molecular weight of nephrin, without postranslational modifications, is 135 kDa (20).

By using these antibodies, nephrin was localized to glomeruli of newborn human kidney cortex by immunofluorescence microscopy (Fig. 2). Immunoreactivity was observed in the GBM region, whereas the podocyte cell bodies, as well as endothelial and mesangial cells, were negative. No specific reactivity of these antibodies against other kidney structures could be detected when compared with preimmune serum (not shown). These results agree with our previous *in situ* hybridization data showing specific expression of the nephrin gene in visceral epithelial cells (podocytes) of human glomeruli (21). The present immunostaining pattern, together with the pre-

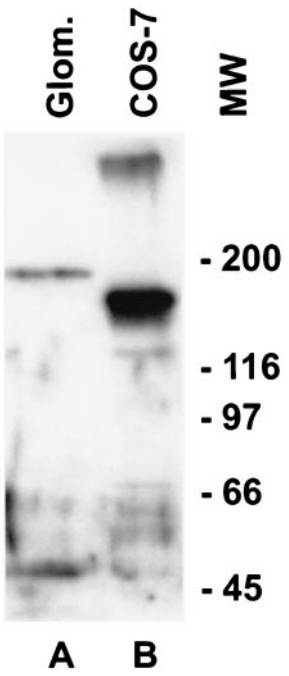

FIG. 1. Western blot analysis of glomerular and recombinant nephrin. A polyclonal anti-nephrin antibody reacts with a 180-kDa protein in a Triton X-100 extract of isolated normal human glomeruli (*A*) and with a 150-kDa protein from the lysate of COS-7 cells transiently transfected with full length nephrin cDNA (*B*). An additional band of over 300 kDa in the front of the gel can also be seen in the COS-7 cell extract. The nonreduced sample from human glomerular extracts did not reveal any immunoreactive bands, indicating extensive disulfide crosslinking of nephrin, and only the 300-kDa band from COS-7 cell extract was present (not shown). The preimmune serum did not reveal any staining (not shown).

vious *in situ* hybridization results, suggests that the transmembrane protein nephrin is located in the podocyte–GBM interface and/or in the slit diaphragm between the podocyte foot processes.

Localization of Nephrin to the Glomerular Slit Diaphragm by Immunoelectron Microscopy. To more precisely determine the location of nephrin, postembedding immunoelectron microscopy was carried out. Affinity-purified rabbit anti-nephrin IgG was found to give much less background staining than did anti-nephrin serum. With the purified IgG against the extracellular fragment of nephrin, immunogold label was, in practice, exclusively found in the podocyte slit diaphragm region between the podocyte foot processes (Fig. 3). In cross sections of the GBM (Fig. 3 *A* and *D*), one or two gold particles, in general, could be detected approximately in every fifth to tenth foot process interspace. Rarely, gold label could be observed in the cytoplasm of a foot process. No label was seen between the podocyte foot processes and the GBM. Neither endothelial nor mesangial cells were labeled. With the protocol used, background labeling with the affinity-purified anti-nephrin IgG was practically absent. In the more parallel sectioned

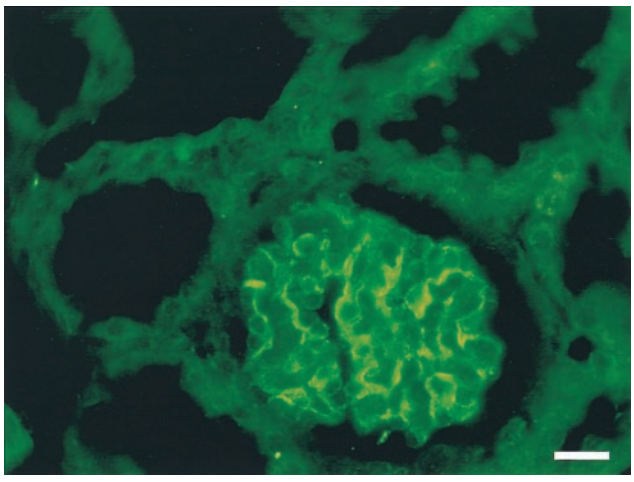

FIG. 2. Immunohistochemical localization of nephrin in human kidney. Immunofluorescence staining was carried out on a 2-mo-old human kidney with antibodies against recombinant human nephrin. Immunoreactivity is seen in the glomerulus, presumably at the podocyte-GBM junction. No staining is present in mesangial or endothelial cells. Bar = 20 nm.

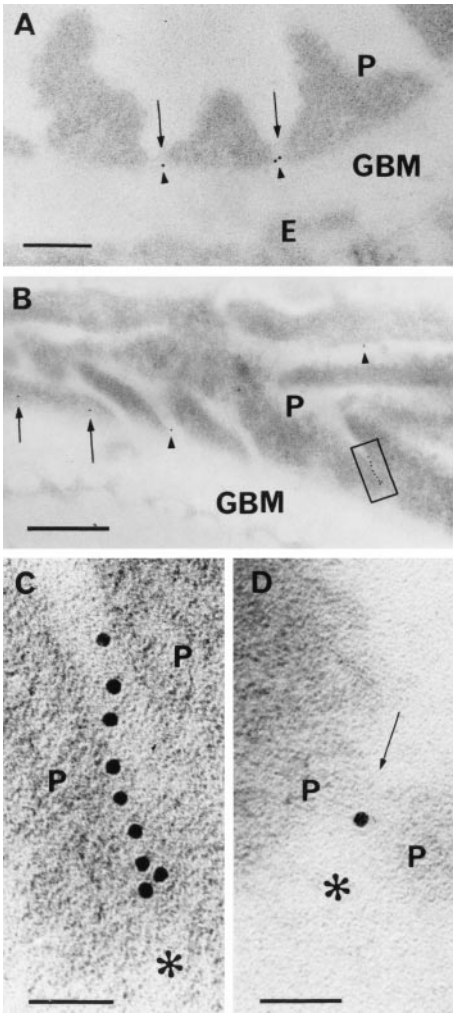

FIG. 3. Immunoelectron microscopic localization of nephrin in human renal glomeruli. Indirect postembedding staining for nephrin by using affinity purified IgG against extracellular region of recombinant human nephrin and 10 nm gold-coupled secondary antibody. (*A*) Paraformaldehyde (PF)-fixed kidney embedded in Lowicryl. Note gold label (arrowheads) between foot processes of podocytes (P). The label is located in the central area of the slit, between the GBM and the faintly visible slit diaphragm (arrows). Endothelium (E) is unlabeled. Bar = 200 nm. (*B*) Several gold particles in a row (box) can be seen between tangentially sectioned podocyte (P) foot processes. Gold particles in two other podocyte–podocyte interspaces are shown with arrowheads. Apparent intracellular staining of a podocyte (arrows) above GBM could be caused by grazing section of slit. Sample treated as in *A*. Bar = 500 nm. (*C*) Blow-up of *B*. The row of nine gold particles lies in tangentially cut, *ca.* 40-nm-wide slit between two podocytes (P). GBM is marked with asterisk. Bar = 50 nm. (*D*) Gold particle between slit diaphragm (arrow) joining two podocytes (P) and GBM (asterisk) in cross section. Sample fixed in 3.5% PF with 0.01% glutaraldehyde and embedded in LR White resin. Bar = 50 nm.

GBM areas, several (up to nine) gold particles could be observed in a slit (Fig. 3 *B* and *C*). In such areas, gold particles could be arranged into single or multiple rows, usually in the center of the slit, as judged by tilting of the sample. Multiple gold particles were not an exceptional finding in slit regions of oblique or tangential sections. With increasing glutaraldehyde concentrations, better ultrastructure but reduced label was seen. Immunogold staining with affinity-purified preimmune serum IgG, with an equivalent protein concentration, was negative (not shown).

DISCUSSION

The remarkable interdigitating pattern of adjacent podocyte foot processes in the kidney glomerulus has implied an essential role of the podocytes for the integrity of the glomerular filtration barrier (27–29). Much interest in the study of this barrier has been focused on the cell junction between the foot processes, the so-called slit diaphragm. However, the actual molecular structure of the diaphragm remains still to be unraveled. In this study, we describe the generation and characterization of antibodies made against nephrin, the product of the gene mutated in patients with congenital nephrotic syndrome NPHS1. Based on its primary structure, nephrin is most likely a signaling adhesion molecule belonging to the Ig superfamily. The present results, showing strong immunostaining of the GBM region in light microscopy and localization of nephrin to the slit diaphragm region by immunoelectron microscopy, provide the first evidence for the presence of a specific protein at this putative size-selective filter of the kidney. The fact that mutations in the nephrin gene lead to massive proteinuria (20, 21) furthermore indicates that nephrin has a direct role or actual filtration function in this size-selective barrier.

Concerning nephrin localization, it should be stressed that, in its extracellular labeling, nephrin was found only between the foot processes. It was conspicuously lacking from the interspaces between the foot processes and the GBM, a site with very much larger potential labeling surface than is present in the narrow slit. The possible deviation of the antigenic epitope from the visible gold label, by using the rabbit anti-nephrin/gold $F(ab)_2$ anti-rabbit complex, can be estimated to be up to 1.5× length of the IgG molecule (30), i.e. about 15 nm. Therefore, the precise molecular location and orientation of nephrin in the approximately 35–45-nm-wide slit remains to be determined. However, some clues are now available from the present results. In some cases, rows up to nine gold particles long were found in favorable tangential sections (Fig. 3 *B* and *C*). This suggests that a linear array of antigenic sites parallel to the GBM surface would exist at some height along the slit, possibly in the slit diaphragm itself. The gold particles on the IgG complexes might, however, line up also under the influence of other molecular determinants in their surroundings.

The occasional cases of gold label observed in the cytoplasm of foot processes, if not the result of tangential sectioning, may represent newly synthesized nephrin molecules. The labeling intensity with the method used in this study was not expected to be very high, as the antibodies were directed only against a small, maybe often unexposed, portion of nephrin. Therefore, the finding of label in only 10–20% of the slits in the ultrathin cross sections is not surprising. Our preliminary results with immunogold- labeled cryosections reveal a higher labeling intensity of the slit diaphragm between well-preserved podocyte foot processes.

The present results raise the fundamental question of how a protein like nephrin, either alone or together with other slit membrane protein(s), can contribute to the molecular structure of a porous filter. The ultrastructure of the podocyte slit diaphragm has been studied extensively by electron microscopy (27). Rodewald and Karnovsky (31) were the first to

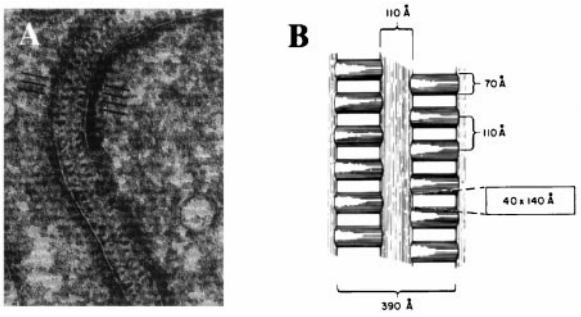

FIG. 4. Morphological structure of the glomerular podocyte slit diaphragm. Reproduced and modified from R. Rodewald and M. J. Karnovsky (31) [reproduced from *The Journal of Cell Biology* (1974) **60,** 423–433, by copyright permission of The Rockefeller University Press]. (*A*) Electron microscopy of tannic acid-stained and glutaraldehyde-fixed rat glomerulus reveals the presence of a central filament and cross bridges. Density of the cytoplasm opposite the points of attachment of the slit diaphragm can be observed. Discontinuities in the diaphragm represent regions where the diaphragm has left the plane of section. (*B*) Schematic model of the slit diaphragm. The average cross section dimensions of the pores between cross bridges are indicated within the rectangle.

suggest a zipper-like organization of this structure (Fig. 4). Because these studies used the conventional thin-sectioning method requiring harsh chemical treatments in sample preparation, it has later been suggested that the zipper-looking structure might be due to an artifact. Since then, the podocyte–podocyte junction has also been studied by several other electron microscopic methods (32, 33). These studies have indicated that the width of this junction varies between 20 and 50 nm. The actual slit diaphragm is considered to be a rather rigid structure. However, it has recently been suggested that at least the slit area might increase with increasing perfusion pressures of the glomerulus (34, 35). Because the actual molecular structure of the slit diaphragm is, as yet, unresolved, it is premature to speculate on a molecular assembly allowing change in the width of the slit. Our results, however, provide evidence that nephrin is a component of such an assembly.

Several lines of evidence indicate that nephrin may assemble into a zipper-like isoporous filter structure similar to that presented by Rodewald and Karnovsky (ref. 31; Fig. 4). First, the present study demonstrated that nephrin is specifically located at the slit diaphragm. Second, nephrin must be crucial for the structural integrity of the slit diaphragm, as absence of the protein or different amino acid substitutions cause congenital nephrosis and lack of the slit diaphragm with massive proteinuria as a result (21). Third, nephrin molecules extending toward each other from two adjacent foot processes are likely to interact with each other in the slit through homophilic interactions, as has been shown for other Ig cell adhesion molecules such as N-CAM (36), C-CAM (37), and L1 (38). Fourth, such homophilic assembly of nephrin molecules in the slit could have a zipper-like arrangement, essentially similar to that proposed based on electron microscopic studies (Figs. 4 and 5).

A hypothetical head-to-head assembly of nephrin through homophilic interactions is illustrated in Fig. 5. The amino terminal extracellular domain of nephrin contains six consecutive Ig repeats, followed by a spacer domain, two additional Ig repeats, and one fibronectin type III-like domain (Fig. 5*A*). Each Ig motif contains two cysteine residues that, similarly to corresponding motifs in other proteins (39), can be assumed to form a disulfide bridge within the repeat structure (Fig. 5*A*). Ig motifs have been shown to adopt a globular or ellipsoid structure with an average axis length of between 24 and 47 Å, averaging 35 Å (40). If the Ig repeats were to form a chain-like structure, as has been proposed for Ig cell adhesion molecules,

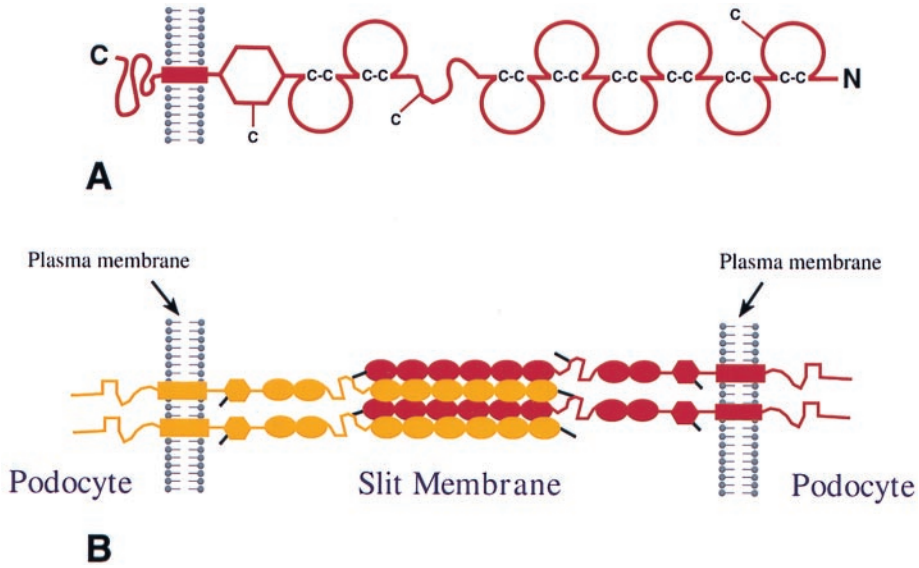

FIG. 5. Hypothetical model of nephrin assembly to form the isoporous filter of the podocyte slit diaphragm. (*A*) Schematic domain structure of nephrin. The Ig repeats are shown by incomplete circles connected by disulfide bridges (C-C). The locations of free cysteine residues are indicated by a —C. (*B*) Possible mode of interdigitating association of four nephrin molecules in the slit between two foot processes. For the sake of clarity, nephrin molecules from opposite foot processes are illustrated in different colors. In this model, it is assumed that Ig repeats 1–6 of a nephrin molecule of one foot process associate in an interdigitating fashion with Ig repeats 1–6 in a neighboring molecule from the opposite foot process. Cysteine residues are depicted by black lines and two potential disulfide bridges crosslinking four nephrin molecules in the center of the slit are illustrated. The remaining single free cysteine present in the fibronectin domain may react with another nephrin molecule, or some other as yet unknown molecule, which may connect with the plasma membrane or cytoskeleton.

all eight motifs would contribute to a length of about 28 nm. The region between Ig repeats 6 and 7 and fibronectin type III-like domain would add more length to the protein. Consequently, a single nephrin molecule can extend through most of the width of the 35- to 45-nm-wide slit diaphragm.

In addition to the two cysteine residues in each Ig motif, nephrin contains three free cysteines, one in Ig motif 1, one in the spacer region between Ig motifs 6 and 7, and one in the fibronectin domain close to the plasma membrane. The three free cysteines are likely to have a function in forming intermolecular disulfide bridges that provide strength to the slit diaphragm. These cysteines are important because their absence results in proteinuria and congenital nephrotic syndrome (21). In the hypothetical model presented here, the free cysteine of Ig motif 1 in one molecule interacts with the cysteine residue of the spacer in another nephrin molecule. Such disulfide bonds could "lock" the homophilic unit of six Ig repeats of one nephrin molecule to similar units of two adjacent nephrin molecules. A centrally located aggregate of numerous nephrin molecules along the slit between two foot processes could constitute the central filament visualized by Rodewald and Karnovsky (31) (Fig. 4*A*). The width of the central aggregate would be 21 nm (6 × 35 Å) by simply assuming a linear chain arrangement of six Ig repeats, 35 Å each, and this would not agree with the 11-nm width of the central filament reported by Rodewald and Karnovsky (31). However, this difference could be attributed to the shrinkage of samples, extraction of components, or failure to stain. Also, the mode of packing of Ig modules may well be different from that presented in the model, so that it is still possible that nephrin forms the basis of the slit diaphragm through homophilic interactions.

In conclusion, the recent identification of nephrin and its present specific localization to the podocyte slit diaphragm may accelerate the elucidation of the molecular structure of the size-selective glomerular filtration barrier. The model for nephrin assembly into a slit diaphragm proposed in this study supports the model for slit diaphragm ultrastructure presented over two decades ago based on transmission electron microscopy. However, further studies are needed to validate this model and examine other proteins contributing to the slit diaphragm structure. Also, other functions of nephrin, such as its potential signaling role, need to be investigated. The elucidation of the molecular structure of the filtration barrier can have significant clinical value. It not only explains the absence of slit diaphragms in NPHS1, but may also help to understand the pathogenic mechanisms of proteinuria in several other genetic and acquired kidney diseases that lead to proteinuria and renal failure. Considering the limited knowledge of the structure of the slit diaphragm, the present results represent a noteworthy advance that may help to unravel the nature of this important extracellular structure.

We thank Riitta Herva for providing human tissue samples for light microscopy. The skillful help of the technical staff in the Electron Microscopy Unit, Institute of Biotechnology, is acknowledged. This work was supported in part by grants from the Sigrid Jusélius Foundation, the Academy of Finland, the Ulla Hjelt Foundation, Helsinki, the Swedish Medical Research Council and Hedlund's Foundation, Stockholm, and the Novo Nordisk Foundation, Copenhagen.

1. Tisher, C. C. & Madsen, K. M. (1996) in *Anatomy of the Kidney*, eds. Brenner, B. M. & Rector, F. C. (Saunders, Philadelphia), Vol. 1, pp. 3–71.
2. Bohrer, M. P., Bayliss, C., Humes, H. D., Glassock, R. J., Robertson, C. R. & Brenner, B. M. (1978) *J. Clin. Invest.* **61,** 72–78.
3. Brenner, B. M., Hostetter, T. H. & Humes, H. D. (1978) *N. Engl. J. Med.* **298,** 826–832.
4. Batsford, S. R., Rohrbach, R. & Vogt, A. (1987) *Kidney Int.* **31,** 710–717.
5. Kanwar, Y. S., Liu, Z. Z. & Wallner, E. I. (1991) *Semin. Nephrol.* **11,** 390–413.
6. Ghitescu, L., Desjardins, M. & Bendayan, M. (1992) *Kidney Int.* **42,** 25–32.
7. Fujigaki, Y., Nagase, M., Kobayasi, S., Hodaka, S., Shimomura, M. & Hishida, A. (1993) *Kidney Int.* **43,** 567–574.
8. Remuzzi, A. & Remuzzi, G. (1994) *Kidney Int.* **45,** 398–402.

9. Yurchenco, P. D. & O'Rear, J. (1993) in *Supramolecular Organization of Basement Membranes*, eds. Rohrbach, D. H. & Timpl, R. (Academy, New York), pp. 19–47.
10. Hudson, B. G., Reeders, S. T. & Tryggvason, K. (1993) *J. Biol. Chem.* **268,** 26033–26036.
11. Caulfield, J. P. & Farquhar, M. G. (1978) *Lab. Invest.* **39,** 505–512.
12. Kanwar, Y. S. & Farquhar, M. G. (1979) *J. Cell. Biol.* **81,** 137–153.
13. Karnovsky, M. J. & Ainsworth, S. K. (1972) *Adv. Nephrol.* **2,** 35–60.
14. Latta, H. (1970) *J. Ultrastruct. Res.* **32,** 526–544.
15. Orikasa, M., Matsui, K., Oite, T. & Shimizu, F. (1988) *J. Immunol.* **141,** 807–814.
16. Kawachi, H., Abrahamson, D. R., StJohn, P. L., Goldstein, D. J., Shia, M. A., Matsui, K., Shimizu, F. & Salant, D. J. (1995) *Am. J. Pathol.* **147,** 823–833.
17. Schnabel, E., Anderson, M. A. & Farquhar, M. G. (1990) *J. Cell. Biol.* **111,** 125512–125563.
18. Kurihara, H., Anderson, J. M. & Farquhar, M. G. (1992) *Proc. Natl. Acad. Sci. USA* **89,** 7075–7079.
19. Rapola, J. (1987) *Pediatr. Nephrol.* **1,** 441–446.
20. Kestilä, M., Lenkkeri, U., Männikkö, M., Lamerdin, J., McCready, P., Putaala, H., Ruotsalainen, V., Morita, T., Nissinen, M., Herva, R., *et al.* (1998) *Mol. Cell* **1,** 575–582.
21. Lenkkeri, U., Männikkö, M., McCready, P., Lamerdin, L., Gribouval, O., Niaudet, P., Antignac, C., Kashtan, C. E., Holmberg, C., Olsen, A., *et al.* (1999) *Am. J. Hum. Genet*. **64,** 51–61.
22. Autio-Harmainen, H. (1981) *Acta Pathol. Microbiol. Scand.* **89,** 215–222.
23. Autio-Harmainen, H. & Rapola, J. (1983) *Nephron* **34,** 48–50.
24. Peränen, J. (1992) *BioTechniques* **13,** 546–549.
25. Laemmli, U. K. (1970) *Nature (London)* **227,** 680–685.
26. Towbin, H., Staehelin, T. & Gordon, J. (1979) *Proc. Natl. Acad. Sci. USA* **76,** 4350–4354.
27. Mundel, P. & Kriz, W. (1995) *Anat. Embryol.* **192,** 385–397.
28. Kriz, W., Hackenthal, E., Nobiling, R., Sakai, T. & Elger, M. (1994) *Kidney Int.* **45,** 369–376.
29. Daniels, B. (1993) *Am. J. Nephrol.* **13,** 318–323.
30. Valentine, R. C. & Green, N. M. (1967) *J. Mol. Biol.* **27,** 615–617.
31. Rodewald, R. & Karnovsky, M. J. (1974) *J. Cell. Biol.* **40,** 423–433.
32. Furukawa, T., Ohno, S., Oguchi, H., Hora, K., Tokunaga, S. & Furuta, S. (1991) *Kidney Int.* **40,** 621–624.
33. Ohno, S., Hora, K., Furukawa, T. & Oguchi, H. (1992) *Virchows Arch. B. Cell. Pathol. Incl. Mol. Pathol.* **61,** 351–358.
34. Yu, Y., Leng, C. G., Kato, Y. & Ohno, S. (1997) *Nephron* **76,** 452–459.
35. Kriz, W., Kretzler, M., Provoost, A. & Shirato, I. (1996) *Kidney Int.* **49,** 1570–1574.
36. Kiselyov, V. V., Berezin, V., Maar, T. E., Soroka, V., Edvardsen, K., Schousboe, A. & Block, E. (1997) *J. Biol. Chem.* **272,** 10125–10134.
37. Öbrink, B. (1997) *Curr. Opin. Cell. Biol.* **9,** 616–626.
38. Sonderegger, P. & Rathjen, F. G. (1992) *J. Cell. Biol.* **119,** 1387–1394.
39. Chothia, C. & Jones, E. Y. (1997) *Annu. Rev. Biochem.* **66,** 823–862.
40. Holden, H. M., Ito, M., Hartshorne, D. J. & Rayment, I. (1992) *J. Mol. Biol.* **227,** 840–851.